Coherent tunneling and negative differential conductivity in graphene-hBN-graphene heterostructure.

Luis Brey
*Instituto de Ciencia de Materiales de Madrid, CSIC, 28049 Cantoblanco, Spain**
(Dated: March 28, 2014)

We address the tunneling current in a graphene-hBN-graphene heterostructure as function of the twisting between the crystals. The twisting induces a modulation of the hopping amplitude between the graphene layers, that provides the extra momentum necessary to satisfy momentum and energy conservation and to activate coherent tunneling between the graphene electrodes. Conservation rules limit the tunneling to states with wavevectors lying at the conic curves defined by the intersection of two Dirac cones shifted in momentum and energy. There is a critical voltage where the intersection is a straight line, and the joint density of states presents a maximum. This reflects in a peak in the tunneling current and in a negative differential conductivity.

arXiv:1403.6073v2 [cond-mat.mes-hall] 27 Mar 2014

Introduction. The same techniques used for obtaining graphene layers[1] can also be applied to obtain two-dimensional (2D) crystal structures of highly anisotropic materials as hexagonal Boron Nitride (hBN)[2] or transition metal dichalcogenides[3]. Once isolated, atomic layers of different 2D crystals can be reassembled layer by layer to create heterostructures with the designed electrical properties[4]. In this direction, recently graphene-hBN-graphene[5–7] and graphene-WS_2[8] heterostructures have been realized and proved as prototype graphene based field-effect tunneling transistors. At high voltages the graphene-hBN-graphene structure shows a negative differencial conductance[7] that has potential applications for logic devices.

Conservation of energy and momentum prevents finite voltage coherent tunneling between 2D-electron gases with circular symmetric dispersion. Coherent tunneling only occurs when the Fermi surfaces of the electron gases are closely aligned[9].

In this work we show that in graphene-hBN-graphene (G-BN-G) heterostructures, the lattice mismatch between graphene and hBN induces an unavoidable twisting and a spatial modulation of the hopping amplitude between the graphene electrodes. This translates into a coherent tunneling current between the graphene layers and a negative differential conductivity. We find that even in the case of perfect crystal arrangement between the graphene layers, the always present misalignment between graphene and hBN, makes possible coherent tunneling between the graphene electrodes.

Geometry and Model. We consider a trilayer structure consisting of top (T) and botton (B) graphene monolayers separated by L monolayers of hBN. T and B graphene layers are rotated angles θ_T and θ_B respectively with respect the central hBN layers, and they have a lattice parameter mismatch δ=1.8% with hBN. For small twisting angles, the tunneling amplitude between the layers varies over distances much larger than the lattice constant and electronic states in Dirac points $\mathbf{K}$ and $\mathbf{K}'$ are effectively decoupled. Therefore we describe each valley separately. Near the Dirac point, $\mathbf{K}=(k_D,0)$ with $k_D=\frac{4\pi}{3a}$, the Hamiltonians for the T and B graphene layers are[10],

$$h_{\rm k}^{T(B)}=\hbar v_F\begin{pmatrix}0 & ke^{i(\theta_{\mathbf{k}}-\theta_{T(B)})}\\ ke^{-i(\theta_{\mathbf{k}}-\theta_{T(B)})} & 0\end{pmatrix} \quad (1)$$

here v_F is the graphene Dirac velocity, $\mathbf{k}$ is the momentum measured from the layer's Dirac point and $\theta_{\mathbf{k}}$ is the angle formed by the momentum with the x-axis. Hamiltonian $h_{\rm k}^{T(B)}$ acts on the amplitude of the wavefunction on the sublattices, A and B, of the graphene layer T(B). The electronic structure of each hBN monolayer is described by a gapful Dirac-like Hamiltonian that acts on the B and N atomic basis,

$$h_{\rm k}^{BN}=\begin{pmatrix}\Delta_1 & \hbar v_{BN}ke^{i\theta_{\mathbf{k}}}\\ \hbar v_{BN}ke^{-i\theta_{\mathbf{k}}} & -\Delta_2\end{pmatrix} \quad (2)$$

where v_{BN} describes the in-plane hopping amplitude between B and N atoms, $\Delta_1+\Delta_2$ is the energy gap of hBN and Δ_1 is the band-offset of the conduction band, Boron-like, of hBN with respect the graphene Dirac point. The different hBN layers are vertically ordered in an eclipse way and the atoms are coupled by a vertical hopping γ_{BN}. This vertical order is a consequence of the bond polarity in hBN.

Top and bottom graphene layers are coupled with the first and last hBN layers through the spatially modulated hopping matrices $V(\theta_T,\delta)$ and $V(\theta_B,\delta)$ respectively, that in the low twisting angle limit have the form[11–13]

$$V(\theta,\delta)=\frac{\hat{t}}{3}\sum_{i=1,3}T_i\,e^{-i\mathbf{q_i}(\theta,\delta)\mathbf{r}}, \quad (3)$$

with $T_1=\begin{pmatrix}1 & 1\\ 1 & 1\end{pmatrix}$, $T_2=\begin{pmatrix}\eta^* & 1\\ \eta & \eta^*\end{pmatrix}$, $T_3=\begin{pmatrix}\eta & 1\\ \eta^* & \eta\end{pmatrix}$, $\hat{t}=\begin{pmatrix}t_{CB} & 0\\ 0 & t_{CN}\end{pmatrix}$ and $\eta=e^{i\frac{2\pi}{3}}$. Being t_{CB} and t_{CN} the C to B and C to N hopping amplitudes respectively. The hopping matrices T_i do not depend on geometrical

* brey@icmm.csic.es

factors. All the information on δ and θ is in the $\mathbf{q_i}$'s.

$$\begin{aligned}
\mathbf{q_1}(\theta,\delta) &= k_D\,(\delta,-\theta)\,,\\
\mathbf{q_2}(\theta,\delta) &= k_D\left(-\frac{\sqrt{3}}{2}\theta+\frac{1}{2}\delta,-\frac{1}{2}\theta-\frac{\sqrt{3}}{2}\delta\right),\\
\mathbf{q_3}(\theta,\delta) &= k_D\left(\frac{\sqrt{3}}{2}\theta+\frac{1}{2}\delta,-\frac{1}{2}\theta+\frac{\sqrt{3}}{2}\delta\right)
\end{aligned} \tag{4}$$

The three wavevectors $\mathbf{q}_i$ have the same modulus and define a periodic hexagonal modulation of the hopping amplitude. This periodicity describes the spatial distribution of the stacking of the graphene C atoms with the B and N atoms of hBN.

Effective Hamiltonian. We obtain an effective bilayer graphene Hamiltonian by integrating out the orbital degree of freedom in the hBN layer,

$$\hat{H}_{\mathbf{k}} = \begin{pmatrix} h^T & 0\\ 0 & h^B\end{pmatrix} + \begin{pmatrix} 0 & \hat{V}\\ \hat{V}^\dagger & 0\end{pmatrix} \tag{5}$$

where,

$$\hat{V} = \hat{t}\,V(\theta_T,\delta)\left(H^{BN}_{\mathbf{k}}\right)^{-1}V(-\theta_B,-\delta)\,\hat{t}\,, \tag{6}$$

and $H^{BN}_{\mathbf{k}}$ is the Hamiltonian of the L layers hBN slab. For wavevectors, $\mathbf{k}$, of the order of the separation between the Dirac points of the T and B graphene layers, $|\mathbf{q}_i|$, the diagonal terms Δ_1 and Δ_2 are the leading contributions in the hBN Hamiltonian $h^{BN}_{\mathbf{k}}$. For those momenta it is a very good approximation to set v_{BN}=0 in $h^{BN}_{\mathbf{k}}$, resulting in the following T to B graphene tunneling modulation,

$$\hat{V} = \frac{1}{9}\sum_{i,j=1,3}\hat{T}_{i,j}\,e^{i\mathbf{G}_{i,j}(\theta_T,\theta_B)\mathbf{r}} \tag{7}$$

with

$$\mathbf{G}_{i,j}(\theta_T,\theta_B) = \mathbf{q}_i(\theta_T,\delta)+\mathbf{q}_j(-\theta_B,-\delta) \tag{8}$$

and

$$\mathcal{T}_{i,j} = \frac{\gamma_{BN}^{L-1}}{(\Delta_1\Delta_2)^L}\,\hat{t}\;T_i\begin{pmatrix}\Delta_2^L & 0\\ 0 & \Delta_1^L\end{pmatrix}T_j\;\hat{t} \tag{9}$$

The three tunneling processes linking T graphene with hBN, combine with the three connecting hBN with B graphene. This results in nine Fourier components of the tunneling modulation between T and B graphene layers. The three *diagonal* wavevectors $\{\mathbf{G}_{ii}\}$ have a modulus G_d=$k_D|\theta_T-\theta_B|$ and vanish when T and B layers are aligned. The six *non-diagonal* transfer momenta have modulus G_{nd}=$k_D\sqrt{\theta_T^2+\theta_B^2+\theta_T\theta_B}$. Therefore, even when the two graphene layers are perfectly aligned, the misalignment with the central hBN layer makes possible tunneling processes between the graphene electrodes. Note that because the T and B graphene layers have the same lattice parameter, the wavevectors $\{\mathbf{G}_{ij}\}$ are independent on the graphene-hBN lattice mismatch, δ.

Tunneling Current in G-BN-G heterostructure. In presence of an applied voltage V, between the T and B graphene electrodes, the tunneling current can be obtained in linear response theory with the tunneling term treated as the perturbation[14].

$$I(V) = \frac{e}{\hbar}g_s g_v\sum_{\substack{\mathbf{k},\{i,j\}\\ \alpha,\beta}}|t_{\alpha,\beta}(\mathbf{k},\mathbf{k}+\mathbf{G}_{ij})|^2\int_{-\infty}^{+\infty}\frac{d\omega}{2\pi}A_\alpha(\mathbf{k},\hbar\omega)A_\beta(\mathbf{k}+\mathbf{G}_{ij},\hbar\omega+eV)\left[n_F(\hbar\omega)-n_F(\hbar\omega+eV)\right], \tag{10}$$

where g_s=2 and g_v=2 account for the spin and valley degeneracy respectively, $\alpha=\pm$ is the band index, $n_F(\epsilon)$=$[\exp((\epsilon-E_F)/k_BT)+1]^{-1}$ is the Fermi factor, $A_\alpha(\mathbf{k},\hbar\omega)$ is the graphene spectral function for band α, and $t_{\alpha,\beta}(\mathbf{k},\mathbf{k}+\mathbf{G}_{ij})$ is the tunneling matrix element between states in the T and B unperturbed graphene layers,

$$t_{\alpha,\beta}(\mathbf{k},\mathbf{k}+\mathbf{G}_{ij}) = \phi^*_\alpha(\mathbf{k})\,\mathcal{T}_{i,j}\,\phi_\beta(\mathbf{k}+\mathbf{G}_{ij})\,, \tag{11}$$

being $\phi_\alpha(\mathbf{k})$=$\frac{1}{\sqrt{2}}\begin{pmatrix}1\\ \alpha e^{i\theta_{\mathbf{k}}}\end{pmatrix}$ the Dirac hamiltonian eigenfunction with momentum $\mathbf{k}$ and energy $\alpha\hbar v_F k$. In the previous expressions E_F is the Fermi energy of the T and B graphene layers that we consider equally doped. In the one electron picture, the spectral function should be proportional to a delta function, in our calculations A_α is approximated by a Lorentzian function centered on the band energy, $\alpha\hbar v_F k$, and with an half width at half maximum $\hbar/\tau$.

The tunneling processes corresponding to different transfer wavevectors $\mathbf{G}_{i,j}$ contribute independently to the current, and because the circular symmetry of the graphene band structure, their contribution to the current only depends on their modulus $|\mathbf{G}_{i,j}|$. Therefore the relevant quantities or the tunneling current are the two modulus G_d and G_{nd}.

It is important to note that there is current between the two graphene layers because they are rotated with respect the central hBN layer. In systems with circular symmetric band structure, only the presence of the unavoidable disorder or phonons make possible the observation of finite voltage incoherent tunneling between two 2D electron gases separated by a barrier. On the con-

trary, in the trilayer G-BN-G heterostructure, the spatial modulation of the hopping amplitude between T and B layers, provides an extra wavevector that make possible the conservation of momentum and energy in the coherent tunneling process.

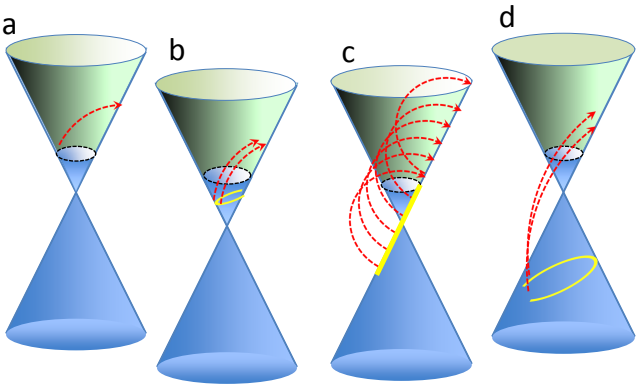

FIG. 1. (Color online)Schematic representation of tunneling processes occurring in the G-hBN-G heterostructure. Blue and green regions mark occupied and empty states respectively. The arrows indicate a tunneling event from the T layer (initial point) to the B layer (end point). These points are shifted in energy by eV. Energy and momentum conservation laws define permitted initial curves in $\mathbf{k}$ space which are plotted in yellow. a) At the minimum voltage for tunneling, only a point in $\mathbf{k}$-space can tunnel, b) by increasing the voltage the conservation curve is an hyperbola that resides in the conduction band, c) at a critical voltage the hiperbola collapses in a straight line and a peak in the joint density of states occurs. d) At larger voltages, the straight line becomes an ellipse, now residing in the valence band.

It is possible to get some insight on the different tunneling contributions analyzing the momentum and energy conservation, together with the Fermi occupation of the T and B layers. In the linear regime, the conduction is different from zero only if the relation $\hbar v_F|\mathbf{G}_{i,j}| < E_F$ is satisfied. That implies finite conductance for twisting angles inside the regions defined by the relations $\hbar v_F k_D|\theta_T+\theta_B| < E_F$ or $\hbar v_F k_D\sqrt{\theta_T^2+\theta_B^2-\theta_T\theta_B} < E_F$. In general, except for very small twist angles, it is appropriated to assume that both G_{nd} and G_d are smaller than k_F and therefore in the linear regime the current is zero.

At finite voltage, energy and momentum conservation define a curve in reciprocal space for the initial tunneling states in the top layer. In general these curves are the conic sections defined by the intersection of two Dirac cones shifted a momentum $\mathbf{G}_{i,j}$ and an energy eV. At small voltages, the tunneling connects conduction band states, and the permitted tunneling wavevectors define an hyperbola. At larger voltages, electrons in the valence band of the top layer can tunnel to the conduction band states of the bottom layer and the allowed momentums form an ellipse. Both hyperbola and ellipse lengths increase with the voltage, and the current should increases continuously with voltage. However, there is a critical voltage where the hyperbola transforms to an ellipse adopting the form of a straight segment. At this critical voltage $V^c=\hbar v_F|\mathbf{G}_{i,j}|$ the cones intersect along two parallel lines and there is a spike in the joint density of states that translates in a peak in the tunneling current. This peak is the origin of the negative differential conductivity in this heterostructure.

The states defined by these conic curves are further limited by the Fermi occupation. That imposes a minimum voltage $V^{min}=\hbar v_F(|\mathbf{G}_{i,j}|-2k_F)$ for the existence of tunneling current. The Fermi occupation also constrains the wavevectors of the states that tunnel at V^c to be in the interval $|\mathbf{G}_{i,j}|$-$k_F < k < k_F$.

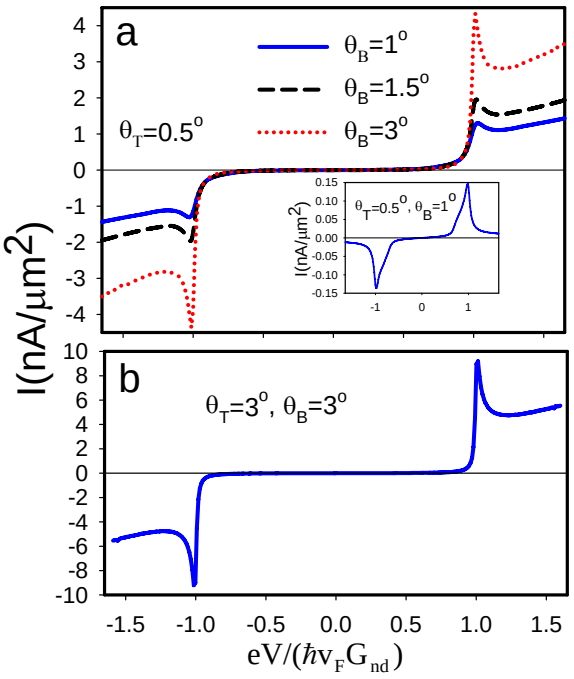

FIG. 2. (Color online)Non-linear current for a graphene-hBN-graphene heterostructure. The density of electrons in both layers is n=5 × 10^{12}cm^{-2}. In panel a) we fix the top layer twist angle to θ_T=0.5^o and plot the current for different rotation angles of the bottom layer θ_B. Both angles are measured with respect the central hBN layer. In the inset we show the conduction to conduction (α=+ to β=+) contribution to the current. In panel b) both graphene layers are rotated the same angle θ_T=θ_B=3^o. The peak in the $I(V)$ indicates that coherent tunneling and negative differential conductivity can occur even when both graphene layers are fully aligned, provided there is a twisting with the hBN layer. In the calculation we use the band structure parameters[15] Δ_1=3.33eV, Δ_2=1.49eV, t_{CB}=0.432eV and t_{CN}=0.29eV and a value $\hbar/\tau$=2.5meV.

Numerical Results. A precise description of the tun-

neling current requires the evaluation of the tunneling matrix elements, Eq.11, which depends on the numerical values of the tight-binding parameters. We have used the band structure parameters recently obtained from *ab initio* calculations by Jung *et al* [15]. In Fig.2 we plot the current for a G-hBN-G heterostructure with different twisting angles. We obtain that at small angles, the tunneling processes associated with the transfer of diagonal momentums $\mathbf{G}_{i,i}$ have a practically null contribution to the current. The main tunneling current is associated with the non diagonal momentum and therefore we measure the bias voltages in units of $\hbar v_F G_{nd}$.

In the inset of the upper part of Fig.2 we show the intraband contribution to the current. The interband contribution is activated at voltage $\hbar v_F(|\mathbf{G}_{nd}|-2k_F)$ and is zero for voltages larger than $V^c=\hbar v_F|\mathbf{G}_{nd}|$). For $V > V^c$ all the tunneling current has its origin in interband processes. Both inter and intraband tunneling show a strong peak at this critical voltage. As discussed above this peak is related to a big increase of the joint density of states occurring at this voltage.

At V^c the interband peak is much stronger than the intraband one. This is because in the intraband tunneling only states with wavevectors in a segment of length k_F contribute the current. However for interband tunneling the number of wavevector contributing to tunneling is proportional to $G_{nd}-k_F$. Then, the strong peak in the $I(V)$ curve is due to valence band to conduction band tunneling processes. In panel a) of Fig.2, we see that as the twisting angles become larger, the value of the momentum transfer increases and with it the intensity of the negative differential peak. Finally the numerical results confirm that the negative differential conductivity peak exists even when both graphene layers are fully aligned, lower panel of Fig.2.

In-plane magnetic field. A magnetic field applied parallel to the graphene layers affects differently to the distinct Fourier components of the interlayer tunneling. Then we expect that the magnetic field splits the negative differential conductivity peak. The experimental observation of this effect would be a definitive indication of the coherent nature of the tunneling.

The magnetic field $\mathbf{B}_\parallel=B_\parallel(\cos\beta,\sin\beta,0)$ is described in the Landau gauge, $\mathbf{A}=B_\parallel(\sin\beta\, z,-\cos\beta\, z,0)$. For isolated graphene layers an in-plane magnetic field shifts the position of the Brillouin zones, and its effect can be cancelled by distinct gauge transformation for the two graphene sheets. Thus, in absence of tunneling the magnetic field has not physical relevance. When electrons can hope between the graphene layers, the motion of the carriers perpendicular to the magnetic field is affected by $\mathbf{B}_\parallel$ [16–18]. and the shift in the k-space reflects in a shift in the tunneling wavevectors,

$$\mathbf{G}_{i,j}\rightarrow\mathbf{G}_{i,j}-\frac{d}{\ell_\parallel^2}(\sin\beta,-\cos\beta) \qquad (12)$$

being $\ell_\parallel=\sqrt{\frac{\hbar c}{eB_\parallel}}$ the magnetic length and d the separation between the graphene ayers. The modulus of the new wavevectors $\mathbf{G}_{i,j}$ depends both on the magnitude of $B_\parallel$ and on the its in-plane orientation.

The position of the peak in the $I(V)$ curve is determined by the modulus of the transfer wavevector. For $B_\parallel$=0 the six non diagonal wavevectors have the same modulus, G_{nd}, and only a peak appears, see Fig.2. The magnetic field modifies the modulus of the transfer wavevectors and the peak in the $I(V)$ curve broadens and splits in presence of $B_\parallel$.

In Fig.3 we plot the effect of $B_\parallel$ on the $I(V)$ peak, for a particular G-hBN-G heterostructure. The negative differential peak splits in three clear peaks, corresponding to three different transfer wavevectors. The other three wavevectors only produce small shoulders only visible in derivates of the curve. The intensity and resolution of the peaks depends on the tunneling amplitude, on the strength of $B_\parallel$, on the modulus of the transfer momentum and on the in-plane orientation of the magnetic field.

In order to observe the effect of the magnetic field, the quantity $d\ell^{-2}$ should be comparable to the value of the modulus of the momentum transfer G_{nd}. This can be achieved by increasing the number of hBN layers or using a very strong magnetic field. The results presented in Fig.3 correspond to just one hBN layer, and the magnetic field corresponding to $d\ell_\parallel^{-2}a$=5 is of the order of $80T$. By increasing the number of hBN layers the separation between graphene layer become larger and the magnetic field required for observing the splitting of the peak should be more accessible.

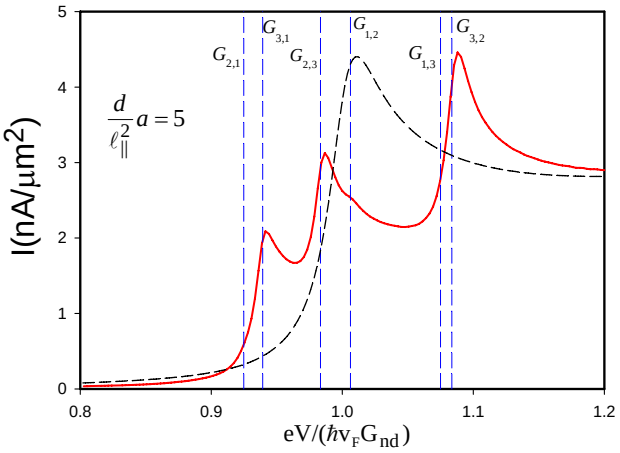

FIG. 3. (Color online)$I(V)$ curve or a G-BN-G structure with twisting angles θ_T=-0.5^o and θ_B=3^o, in presence of an in-plane magnetic field corresponding to $d\ell_\parallel^{-2}a$=5, being a the graphene lattice parameter. The density of carriers in both layers is n=5×10^{1}2cm^{-2}. The current for $B_\parallel$=0 is shown as a black dashed line. Vertical lines indicate the critical voltages corresponding to the different magnetic field modified tunneling transfer wavevectors $\mathbf{G}_{i\neq j}$.

We note that recent field effect tunneling[6] and nega-

tive differential conductance[7] experiments in Gr-hBN-Gr heterostructures have been explained by assuming disorder induced momentum conservation relaxation and therefore non-coherent tunneling. Also, recently Feenstra *et al.*[19] considered the tunneling between n- and p-doped graphene layers separated by a dielectric barrier. That work applied the transfer Hamiltonian formalism to model the tunneling between missoriented graphene layers, and the information on the dielectric crystal structure is neglected.

In summary, we have studied the tunneling current between two graphene layers separated by a hBN layer. The twisting of the layers induces a spatial modulation of the hopping amplitude between the graphene electrodes that provide extra wavevectors to the tunneling process. These extra momenta make possible the conservation of energy and momentum and activates coherent tunneling. Because of the Dirac-like linear dispersion of graphene, the wavevectors that conserve energy and momentum in the tunneling process, can be defined as the intersection of two Dirac cones shifted in momentum and energy. At a critical voltage, the intersection conic curves collapse in a straight segment, and there is a strong peak in the joint density of states and in the tunneling current.

When finishing this work we learnt about the experimental work of K.Novoselov *et al.* where possible signatures of negative differential conductance and coherent tunneling in G-hBN-G heterestructures were reported[20].

ACKNOWLEDGMENTS

This work has been partially supported by MEC-Spain under grant FIS2012-33521. Luis Brey thanks C.Tejedor for a critical reading of the manuscript.

[1] K. S. Novoselov, A. K. Geim, S. V. Morozov, D. Jiang, Y. Zhang, S. V. Dubonos, I. V. Gregorieva, and A. A. Firsov, Science, **306**, 666 (2004).
[2] C.R.Dean *et al.*, Nature Nanotech., **5**, 172 (2010).
[3] K. F. Mak, C. Lee, J. Hone, J. Shan, and T. F. Heinz, Phys. Rev. Lett., **105**, 136805 (2010).
[4] A.K.Geim and I.V.Grigorieva, Nature, **499**, 419 (2013).
[5] G.-H. Lee, Y.-J. Yu, C. Lee, C. Dean, K. L. Shepard, P. Kim, and J. Hone, Applied Physics Letters, **99**, 243114 (2011).
[6] L. Britnell, R. V. Gorbachev, R. Jalil, B. D. Belle, F. Schedin, A. Mishchenko, T. Georgiou, M. I. Katsnelson, L. Eaves, S. V. Morozov, N. M. R. Peres, J. Leist, A. K. Geim, K. S. Novoselov, and L. A. Ponomarenko, Science, **335**, 947 (2012), http://www.sciencemag.org/content/335/6071/947.full.pdf.
[7] L. Britnell, R. V. Gorbachev, A. K. Geim, L. A. Ponomarenko, A. Mishchenko, M. T. Greenaway, T. M. Fromhold, K. S. Novoselov, and L. Eaves, Nature Communications, **4**, 1794 (2013), doi:10.1038/ncomms2817, arXiv:1303.6864 [cond-mat.mes-hall].
[8] T. Georgiou, R. Jalil, B. D. Belle, L. Britnell, R. V. Gorbachev, S. V. Morozov, Y.-J. Kim, A. Gholinia, S. J. Haigh, O. Makarovsky, L. Eaves, L. A. Ponomarenko, A. K. Geim, K. S. Novoselov, and A. Mishchenko, Nature Nanotechnology, **8**, 100 (2013), arXiv:1211.5090 [cond-mat.mes-hall].
[9] J. P. Eisenstein, L. N. Pfeiffer, and K. W. West, Applied Physics Letters, **58** (1991).
[10] A. H. Castro Neto, F. Guinea, N. M. R. Peres, K. S. Novoselov, and A. K. Geim, Rev. Mod. Phys., **81**, 109 (2009).
[11] J. M. B. Lopes dos Santos, N. M. R. Peres, and A. H. Castro Neto, Phys. Rev. Lett., **99**, 256802 (2007).
[12] R. Bistritzer and A. H. MacDonald, PNAS, **108**, 12233 (2011).
[13] M. Kindermann, B. Uchoa, and D. L. Miller, Phys. Rev. B, **86**, 115415 (2012).
[14] G. D. Mahan, *Many Particle Physics* (Plenum, New York, USA, 1981).
[15] J. Jung, A. Raoux, Z. Qiao, and A. H. MacDonald, ArXiv e-prints (2013), arXiv:1312.7723 [cond-mat.mes-hall].
[16] R. K. Hayden, D. K. Maude, L. Eaves, E. C. Valadares, M. Henini, F. W. Sheard, O. H. Hughes, J. C. Portal, and L. Cury, Phys. Rev. Lett., **66**, 1749 (1991).
[17] L. Brey, G. Platero, and C. Tejedor, Phys. Rev. B, **38**, 9649 (1988).
[18] V. I. Fal'ko and S. V. Meshkov, Semiconductor Science and Technology, **6**, 196 (1991).
[19] R. M. Feenstra, D. Jena, and G. Gu, Journal of Applied Physics, **111**, 043711 (2012).
[20] Bulletin of the American Physica Society, APS March Meeting 2014. Session T39.